Acta Cryst. (1979). A**35**, 468–475

Determination of Secondary-Extinction-Free Values for the Flipping Ratio in Polarized Neutron Diffraction

By B. van Laar

Netherlands Energy Research Foundation ECN, Petten (NH), The Netherlands

F. Maniawski

Institute of Nuclear Physics, IFJ, Kraków, Poland

and S. Kaprzyk

Academy of Mining and Metallurgy, AGH, Kraków, Poland

(*Received* 20 *November* 1978; *accepted* 2 *January* 1979)

Abstract

In the analysis of data obtained by polarized neutron scattering, corrections for extinction are of vital interest. It is demonstrated that, in some materials like metal alloys, secondary extinction in samples obtained from ingots by standard methods is very unlikely to be described by a simple mosaic model. It is shown that cold working of the samples improves the sample properties in this respect. Examples of such treatment are given and a method is described to analyse R-on-rocking-curve data in order to obtain data corrected for secondary extinction.

1. Introduction

For the determination of the magnetic-moment density on an atomic scale in magnetic materials, the diffraction of polarized neutrons by magnetized samples is a well-known tool. This method utilizes the coherence that can occur between nuclear and magnetic scattering in Bragg peaks when certain experimental conditions are fulfilled. One of these conditions is that the neutrons in the incident beam all have the same spin state, parallel or anti-parallel to the magnetization direction of the sample. During the experiment, diffracted intensities are collecting for both incoming spin states of neutron polarization. From the ratio of these intensities, the flipping ratio R, it is in principle possible to calculate the magnetic scattering length of the atoms in the sample, provided that their nuclear scattering length is known. More details of the method are given in Nathans, Shull, Shirane & Andresen (1959).

With the polarized neutron beams that are available nowadays it is often possible to obtain flipping ratios with a statistical accuracy of 1 in 10^4. Thus, the real accuracy of the final result depends on the precision of the corrections for various effects that have to be applied to the raw data. One of these effects is the presence of secondary extinction. A method that can be used for the detection of occurrence of secondary extinction is the R-on-rocking-curve method. This method utilizes the fact that the magnitude of the scattering power of a given crystal, and hence the degree of extinction, is changed by reversing the direction of the incident neutron polarization without altering the sample. By recording the flipping ratio R as the crystal is rotated through the Bragg peak, an indication of the presence of secondary extinction may be obtained in those cases where the width of the rocking curve is mainly governed by the orientation spread in the crystal and not by the divergence of the primary beam. When this condition is fulfilled, one may expect that in the Bragg peak, where the scattering is maximum, the extinction effects are most pronounced. As the crystal is rotated off the peak, fewer volumes in the crystal will be in reflecting position and R will be less affected by extinction.

From these considerations one expects the following behaviour for R in the absence of any scattering other than Bragg scattering for an ideally imperfect crystal, *i.e.* a crystal consisting of perfect mosaic blocks which have some regular orientational spread.

At the maximum of the symmetric rocking curve, R is minimum. When the crystal is rotated off the maximum in either direction R increases and approaches the limit of extinction-free R. This behaviour is visualized in Fig. 1. The magnitude of the dip in R depends on various properties of the crystal, such as scattering cross-section, thickness, mosaic spread, but qualitatively the picture should be general.

A method as described above has been used by Nathans, Shull, Shirane & Andresen (1959) for investigating samples of Fe of various thicknesses in the presence of secondary extinction. These authors found

0567-7394/79/030468-08$01.00

that the rocking curve of the 110 reflection of an Fe sample with a thickness of 1·25 mm shows a behaviour as presented in Fig. 1. The observed R at the maximum of the Bragg peak was about 2·2 whereas a value of 3·7 was found when the crystal was rotated sufficiently far from this maximum. In a similar experiment, performed on a thinner sample (0·41 mm), they observed a constant value (3·7) for R over the whole angular range. From this it was concluded that the thinner sample was already free of secondary extinction.

Another example is given (Lander & Brun, 1973; Brun & Lander, 1974) in a study of the magnetic form factor of Tb in $Tb(OH)_3$. In this investigation it was concluded that the flipping ratio was independent of the intensity and that the extinction is primary or secondary, of type II. Unfortunately, the data presented in Brun & Lander (1973) are not accurate enough to justify these conclusions.

The importance of the extinction effect in polarized neutron diffraction has been demonstrated by Bonnet, Delapalme, Becker & Fuess (1976). These authors demonstrated that in yttrium iron garnet (YIG), extinction could be described by an analytical model in which some parameters have to be fitted. However, the conditions met in YIG may not be true in non-ionic samples like metals or alloys, for which it is known that the history of growth, slicing, and mechanical shaping has an effect, very often strongly anisotropic, on the microproperties that are fundamental for extinction.

To our knowledge, no study has been reported in which the quantitative behaviour of the flipping ratio R-on-rocking-curve has been used to infer a quantitative value for the amount of secondary extinction and to deduce a value for R, corrected for this phenomena. Since in polarized neutron experiments, extinction corrections are most troublesome, it seemed worth while to investigate the possibility of the deduction of information about extinction from the R-on-rocking-curve in more detail. Experiments were performed on samples of Ni-rich Ni–V alloys. Results of this investigation are reported in this paper.

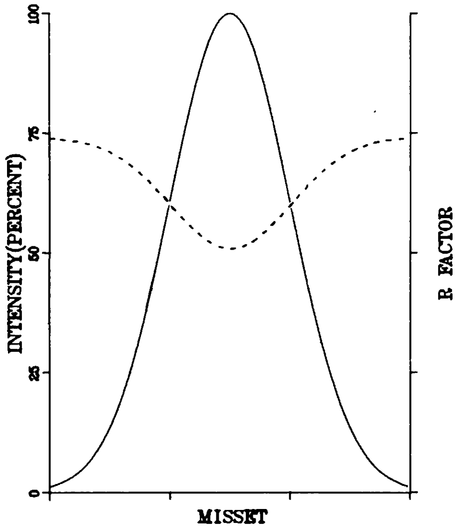

Fig. 1. Expected rocking curve (solid line) and flipping ratio R (broken line) in the case of an ideally imperfect crystal.

2. General

The idea of deducing more quantitative information about extinction from the behaviour of the flipping ratio on various points of the rocking curve implies already the assumption that the amount of extinction is directly related to the intensity scattered by the sample. At various points of the rocking curve the scattering by the sample is different (related to its mosaic distribution) and therefore the amount of extinction varies. In order to deduce from the data a value for the flipping ratio, corrected for extinction, it is necessary to describe the quantitative relation between scattered intensity and amount of extinction.

In this phenomenological approach, it is not yet necessary to use any particular model for the extinction process itself. It is only required that there should exist a one-to-one correspondence between scattered intensity and the amount of extinction. The extinction-free value for R then should follow from extrapolation of the observed intensities to zero.

In the following it is assumed that the observed scattered intensity from the crystal at a misset angle ε is composed of an intensity $I_B(\varepsilon)$ because of Bragg scattering and a non-Bragg background $I_N(\varepsilon)$. The observable flipping ratio is then

$$R(\varepsilon) = \frac{I_B^+(\varepsilon) + I_N^+(\varepsilon)}{I_B^-(\varepsilon) + I_N^-(\varepsilon)}, \quad (1)$$

with

$$R_B(\varepsilon) = \frac{I_B^+(\varepsilon)}{I_B^-(\varepsilon)}, \quad (2a)$$

$$R_N(\varepsilon) = \frac{I_N^+(\varepsilon)}{I_N^-(\varepsilon)}, \quad (2b)$$

then

$$R(\varepsilon) = R_B(\varepsilon) \frac{I^+(\varepsilon)}{I^+(\varepsilon) + I_N^+(\varepsilon)[R_B(\varepsilon)/R_N(\varepsilon) - 1]}, \quad (3)$$

where

$$I^+(\varepsilon) = I_B^+(\varepsilon) + I_N^+(\varepsilon).$$

With the definitions

$$p(\varepsilon) = \frac{I^+(\varepsilon)}{I^+(0)}, \quad (4a)$$

$$\beta(\varepsilon) = \frac{I_N^+(\varepsilon)}{I^+(0)}, \quad (4b)$$

one obtains

$$R(\varepsilon) = R_B(\varepsilon)\frac{p(\varepsilon)}{p(\varepsilon) + \beta(\varepsilon)[R_B(\varepsilon)/R_N(\varepsilon) - 1]}. \quad (5)$$

Equation (5) describes the behaviour of the flipping ratio $R(\varepsilon)$ when a crystal is rocked around its Bragg position in terms of $R_B(\varepsilon)$, the flipping ratio for Bragg scattering which is still affected by extinction, $R_N(\varepsilon)$ which describes the polarization dependence of the background, and the two parameters $p(\varepsilon)$ and $\beta(\varepsilon)$ which describe the angular dependence of total and background scattering respectively.

Now, the simpler case is considered in which the non-Bragg background is non-polarized and much less dependent on ε than the Bragg scattering. In most experimental studies of Bragg scattering this condition will be met.

Then

$$\beta(\varepsilon) = \beta, \quad R_N(\varepsilon) = 1,$$

and

$$R(\varepsilon) = R_B(\varepsilon)\frac{p(\varepsilon)}{p(\varepsilon) + \beta[R_B(\varepsilon) - 1]}. \quad (6)$$

When no extinction is present, $R_B(\varepsilon)$ is constant and equal to R. The presence of extinction will cause a deviation of $R_B(\varepsilon)$ from R,

$$R_B(\varepsilon) = R\,\Psi[I_B^+(\varepsilon)]. \quad (7)$$

If a mathematical form of Ψ were known, (6) could be used for obtaining the desired value for R from a fit to the observed $R(\varepsilon)$ values.

At this point, we remark that deducing a general analytical expression for $R_B(\varepsilon)$ for a non-ideal crystal will be difficult, if not impossible, because properties that are responsible for extinction in a crystal may generally not be analytically descriptive and in addition, they may vary in an unpredictable way from sample to sample. Some further considerations concerning the form of Ψ are given in the Appendix.

3. Experimental

The polarized neutron beam diffractometer COPOL, on which all measurements were performed was installed at the HFR reactor at Petten, The Netherlands. This diffractometer has been made operational in collaboration with the Institute of Nuclear Physics, IFJ, Kraków, Poland. The polarization of the monochromatic beam is $\geq 99\%$, the wavelength is 1·08 Å and the flipping efficiencies of the two spin flippers are $\geq 99{\cdot}9\%$.

Ingots of $Ni_{1-x}V_x$ (x = 0·017 and 0·053) were grown by the Bridgeman method. Oriented ingots were sliced with a mechanical wire saw using abrasive powder of grade 600. The same grade powder was used for smoothing the surfaces of the slices on a flat table. Final finishing was by electropolishing (~0·050 mm deep) at room temperature. The thinnest samples were obtained by one-side electropolishing of 0·20 mm thick samples glued to an aluminium backing with a resin cement. All samples were plane-parallel discs with a diameter of 24 mm.

For the measurements shown in Figs. 2 and 3, samples of thickness 0·190 mm and 0·065 mm, respectively, were used. The sample used for the measurements of Figs. 4 and 5 had a thickness of ~0·005 mm.

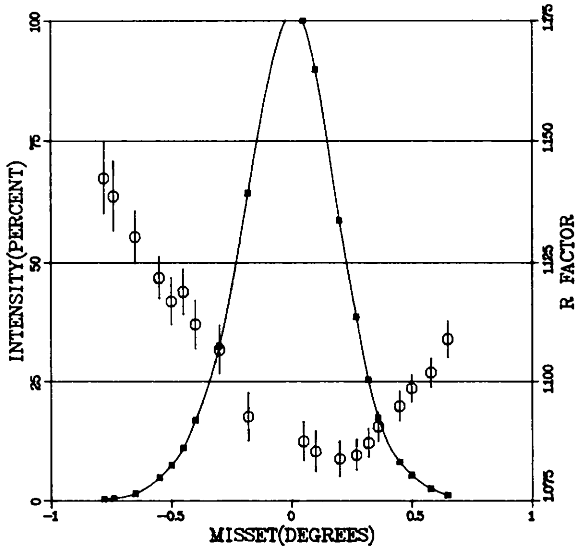

Fig. 2. Observed rocking curve (full line) and R factor, $R(\varepsilon)$ (open circles); $0\bar{2}\bar{2}$ in symmetric reflection, sample $Ni_{0.947}V_{0.053}$, t = 0·190 mm.

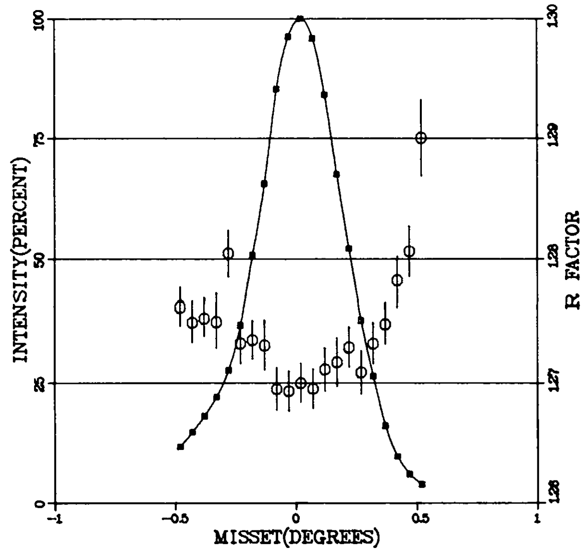

Fig. 3. Observed rocking curve and R factor; $\bar{1}\bar{1}1$ in symmetric transmission, sample $Ni_{0.947}V_{0.053}$, t = 0·065 mm.

Some samples prepared in the above way were given further treatment consisting of subsequent cold-work, annealing, smoothing and electropolishing.

Thus sample 1 used for Fig. 6 was bent 1500 times on a cylinder of radius 70 mm, when having a thickness of 0·440 mm. Care was taken that each bend was carried out along a different direction. After this, thinning on a flat table was done, following by electropolishing to reach the final thickness of 0·150 mm.

Sample 2*A*, for Figs. 7 and 8, was bent 1500 times on a cylinder of radius 15 mm and annealed for two hours at 973 K. No further finishing was applied. Its thickness was 0·10 mm.

Sample 3, for Figs. 9 and 10 was treated similarly to sample 1 except that the bending was performed on a cylinder of radius 25 mm and, after bending, annealing was carried out for 22 h at 873 K.

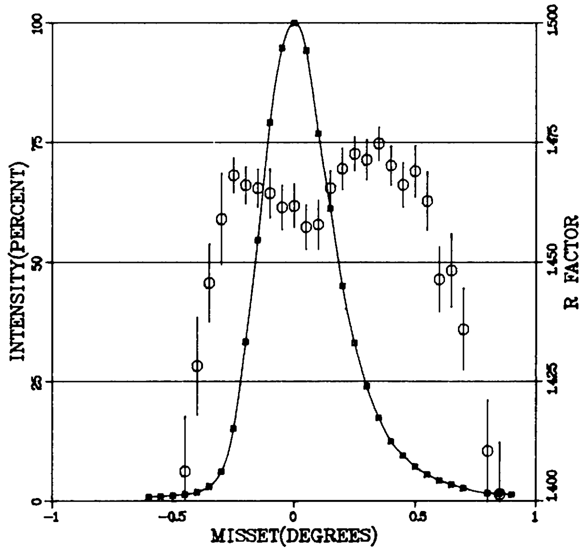

Fig. 4. Observed rocking curve and *R* factor; $11\bar{1}$ in transmission, sample $Ni_{0.983}V_{0.017}$, $t = 0{\cdot}005$ mm.

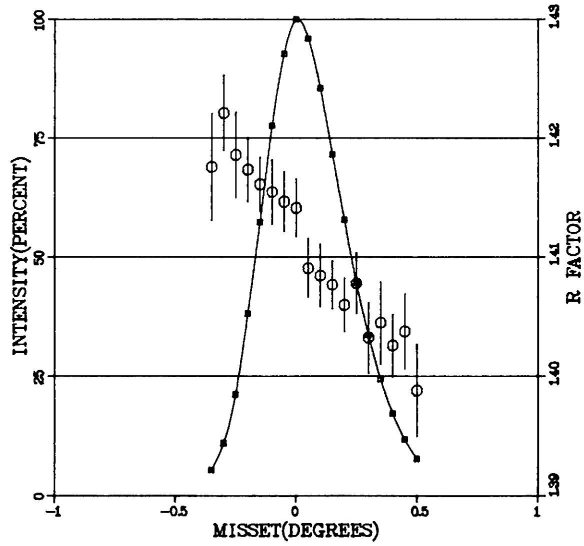

Fig. 5. Observed rocking curve and *R* factor; 020 in symmetric transmission, sample $Ni_{0.983}V_{0.017}$, $t = 0{\cdot}005$ mm.

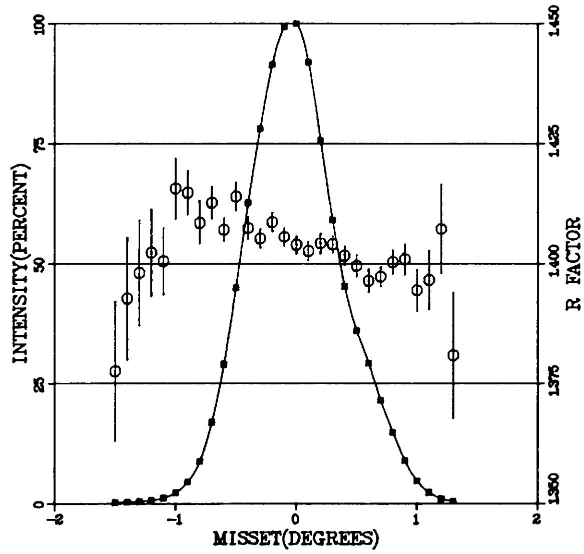

Fig. 6. Observed rocking curve and *R* factor; 200 in symmetric transmission, sample 1, $Ni_{0.983}V_{0.017}$, t = 0·150 mm, cold-worked.

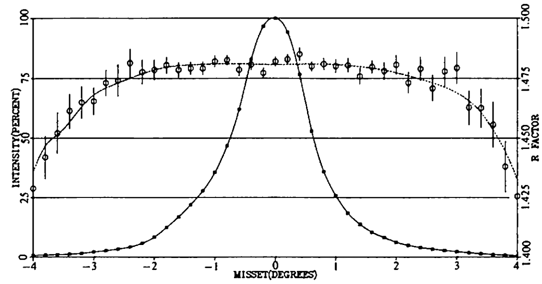

Fig. 7. Observed rocking curve and *R* factor $1\bar{1}\bar{1}$ in symmetric transmission, sample 2*A*, $Ni_{0.983}V_{0.017}$, t = 0·10 mm, cold-worked. The dashed line is the result of the least-squares fit, described in the text.

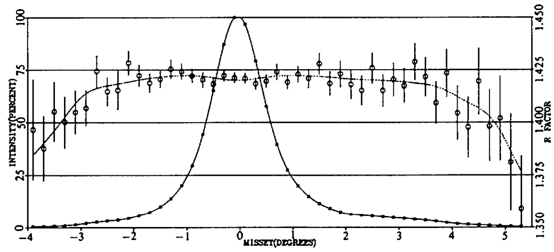

Fig. 8. Observed rocking curve and *R* factor; 200 in symmetric transmission, sample 2*A*, $Ni_{0.983}V_{0.017}$, t = 0·10 mm, cold-worked.

4. Rocking curves of non-cold-worked samples

In Figs. 2–5 the rocking curves and the corresponding flipping ratios are given for different reflections for two compositions of the alloy and variable thickness of the samples. The samples were prepared (as described in the next part of this paper) directly from the ingots avoiding as far as possible any damage of the ingot's microstructure.

From the presented data it is clear that no simple isotropic model, *e.g.* that described by Zachariasen (1967), can be used to describe the strongly irregular behaviour of $R(\varepsilon)$. Even for an extremely thin sample (thickness 0·005 mm), extinction was noticeable. The observed irregularities must be ascribed to features of the individual samples cut from an ingot and are connected to both the growth history of the ingot and to the mechanical treatment each sample has received. The common feature of the curves is a general lack of the desired one-to-one correspondence between observed intensity and observed R-factor. This is a very striking feature because all possible extinction models will have one thing in common; the same amount of scattered intensity has to be related to the same amount of extinction. Therefore, it is impossible *a priori* to explain the observations presented in Figs. 2–5, on the basis of some extinction model and no attempt can be made to deduce an extinction-free value for the flipping ratios. At this point the question may be raised whether any other method used for quantitative estimation of extinction-free R values, like for instance measurements of the wavelength dependence of $R(0)$, the peak value of $R(\varepsilon)$, and subsequent extrapolation to zero wavelength would be successful when dealing with the present samples. It seems reasonable to answer this question negatively.

Because of these considerations, we have tried not only to decrease the amount of extinction in these materials, but to homogenize the material in such a way that the accidental structure of the observed curves would change qualitatively into that indicated in Fig. 1. This goal seems to be achieved by subsequent cold-working of the samples, followed by annealing on the grounds that a more uniform dislocation pattern would cause a more homogeneous mosaic distribution, thus resulting in a more regular shape of the R-on-rocking-curve.

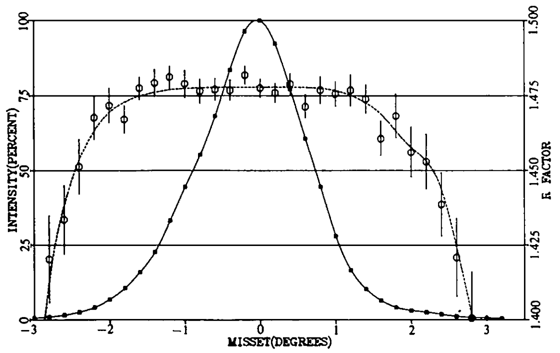

Fig. 9. Observed rocking curve and R factor; $1\bar{1}1$ in transmission, sample 3, $Ni_{0.983}V_{0.017}$, $t = 0{\cdot}143$ mm, cold-worked.

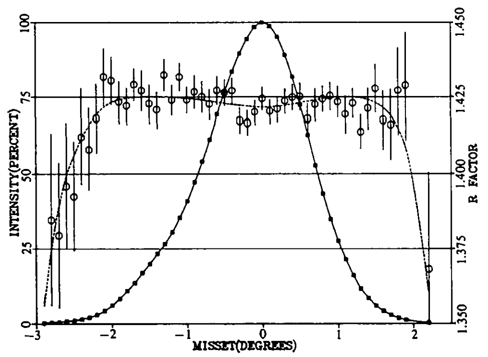

Fig. 10. Observed rocking curve and R factor; 200 in symmetric transmission, sample 3, $Ni_{0.983}V_{0.017}$, $t = 0{\cdot}143$ mm, cold-worked.

5. Rocking curves of cold-worked samples

In Figs. 6–10 R-on-rocking-curve data from the cold-worked samples are given. Fig. 6 clearly shows an improvement compared with the non-cold-worked samples (Figs. 2–5). This improvement refers to both diminution of the amount of extinction and an improved regularity of the R-on-rocking-curve. However, this improvement is not yet satisfactory because the curve in Fig. 6 is not regular enough to be treated analytically.

The curves in Figs. 7–10 show a further improvement which we consider satisfactory enough to enable a reliable analysis to be performed.

Thus, it seems to be possible to deduce an extinction-free R value from the rocking-curve data of a sample that has received a treatment that influenced its microstructural properties to such an extent that a one-to-one correspondence between flipping ratio and intensity has been restored.

The results of measurements on the two strongest reflections of samples 2A and 3 are given in Table 1. For each reflection the following quantities are given: sample number as described previously; α and α', the angles between the normal to the sample surface and the direction of the incident and diffracted beam, respectively (Fig. 11); the effective neutron beam path l

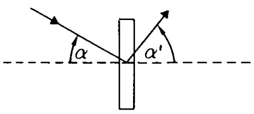

Fig. 11. Definition of the angles α and α' that describe the geometry of incident and diffracted neutron beam with respect to the surface of the samples.

within the sample, defined as $l = \frac{1}{2}d(1/\cos\alpha + 1/\cos\alpha')$ where d is the crystal thickness; and the peak value $R(0)$ of the flipping ratio. The numbers in the last two columns, the extinction-free value R for the flipping ratio and the quantity $[R - R_B(0)]/R$, are obtained by the extrapolation procedure described in the next paragraph.

6. Extrapolation procedure

In order to deduce extinction-free values for R from the data, an extinction correction for Bragg scattering has to be incorporated into (6). This means that the observed R factor for Bragg scattering $R_B(\varepsilon)$ has to be expressed in terms of the extinction-free value R and some parameter(s) describing its dependence on the amount of diffracted intensity.

At this stage, it is in principle possible to introduce any, more or less sophisticated, model that describes the extinction phenomenon. The model that is used in the present paper is the simplest model that can be fitted satisfactorily to the experimental data.

We found, as will be shown below, that a very simple linear expression for the extinction behaviour can be fitted to the observed data. That means that the treatment of the samples described in the previous part of this paper reduced the amount of extinction in the present samples to such an extent that this linear approximation appears to be sufficient.

In this linear approximation we may assume that the amount of extinction is a linear function of scattered intensity. In this case we may write the observed flipping ratio $R_B(\varepsilon)$ as a function of the extinction-free R:

$$R_B(\varepsilon) = R\,\frac{1 - GI_B^+(\varepsilon)}{1 - GI_B^-(\varepsilon)} \approx R[1 - G\Delta I(\varepsilon)], \qquad (8)$$

where

$$\Delta I(\varepsilon) = I_B^+(\varepsilon) - I_B^-(\varepsilon) = I^+(\varepsilon) - I^-(\varepsilon) \qquad (9)$$

and G is a fitting parameter related to the extinction effect in the particular reflection.

Equations (8) and (9) express that the effect of extinction on $R_B(\varepsilon)$ decreases linearly with decreasing intensity difference $\Delta I(\varepsilon)$ and that there is no more extinction when $\Delta I(\varepsilon)$ reaches zero.

Inserting (8) into (6) we obtain

$$R(\varepsilon) = R\,\frac{p(\varepsilon)[1 - G\Delta I(\varepsilon)]}{p(\varepsilon) + \beta\{R[1 - G\Delta I(\varepsilon)] - 1\}}. \qquad (10)$$

Equation (10) describes the variation of the observed flipping ratio $R(\varepsilon)$ when the crystal is rotated through the Bragg position (misset angle ε) when the former assumptions are valid. These assumptions are:

(i) amount of non-Bragg background is constant under the Bragg peak,

(ii) non-Bragg background is unpolarized ($R_N = 1$),

(iii) condition (8) is valid. This condition is discussed in the Appendix.

Expression (10) was used to fit the observed $R(\varepsilon)$ values by a non-linear least-squares method. In this fit, values may be obtained for the extinction-free flipping ratio R together with the parameters G and β, representing the amount of extinction and the non-polarized background respectively.

The results of this fitting are given in Table 1.

7. Results of the extrapolation procedure and discussion

Table 1 shows that values for R obtained from the extrapolation procedure for different equivalent reflections are equal within experimental error, whereas the peak values $R(0)$ are different; the applied correction could also be different in this case. Typical examples of the extrapolation procedure are given in Figs. 7–10. In

Table 1. *Listing of experimental data and data obtained by processing with the extrapolation procedure described in the text of two samples of the alloy* $Ni_{0.983}V_{0.017}$

Reflections marked by an asterisk are visualized in Figs. 7–10.

hkl	Sample no.	α (°)	α′ (°)	Effective path *l* (mm)	*R*(0)	*R*	$\frac{R - R_B(0)}{R}$
$1\bar{1}1$*	3	51	−20	0·189	1·4778 (11)	1·4793 (13)	0·0006 (13)
111	2*A*	15	15	0·104	1·4810 (11)	1·4833 (11)	0·0013 (12)
$1\bar{1}\bar{1}$*	2*A*	15	15	0·104	1·4806 (7)	1·4822 (8)	0·0009 (9)
$1\bar{1}1$	2*A*	39	−70	0·211	1·4749 (11)	1·4819 (10)	0·0046 (11)
$11\bar{1}$	2*A*	70	−39	0·211	1·4734 (12)	1·4828 (11)	0·0058 (12)
200*	3	18	18	0·150	1·4217 (10)	1·4274 (13)	0·0038 (17)
020	3	18	18	0·150	1·4212 (14)	1·4229 (17)	0·0011 (17)
002	2*A*	27	−63	0·166	1·4167 (13)	1·4200 (15)	0·0021 (16)
020	2*A*	63	−27	0·166	1·4145 (12)	1·4231 (14)	0·0057 (15)
200*	2*A*	18	18	0·105	1·4200 (9)	1·4240 (10)	0·0027 (11)

these figures, those reflections are presented that are marked with asterisks in Table 1.

Table 1 also shows that even for geometrically equivalent pairs of reflections, having the same path length l, such as 111 and $1\bar{1}\bar{1}$, $1\bar{1}1$ and $11\bar{1}$, 002 and 020 for sample 2A, or 200 and 020 for sample 3, the applied correction $[R - R_B(0)]/R$ is different. This means that any (known) procedure for extinction correction would have to fail if one attempted to use the procedure to correct peak-value data without a knowledge of the rocking curve behaviour.

The discrepancies in the experimental data for the peak values $R(0)$ cited in Table 1 are most probably caused by simultaneous reflection effects. Nevertheless, R values obtained from the extrapolation procedure are much less sensitive to this effect than the peak values. This may be understood in the following way; R as resulting from the fitting procedure is influenced (with varying statistical weighting factor) by all points on the rocking curve. If only some of these points are affected by simultaneous reflection effects, R will generally be less affected than those individual points. However, it must be admitted that further analysis should be performed in order to determine the size of the simultaneous reflection effect on R, determined in this way. In this paper we will not be concerned further with this phenomenon as correction for extinction is our main aim.

As the phenomena, described in this report, are very likely also to be present in other materials than those used in the present work, it is advisable to explore the situation in materials to be investigated before starting a more or less automatic data collecting program and using a set of R values as input for some data processing procedure that might be based on assumptions and conditions that are not valid for the specimen. In this case, the extrapolation procedure described above may provide a means of obtaining more reliable R values. It is a serious disadvantage that the method is rather time consuming in the data collection stage.

The authors thank Miss J. Kwiatkowska of IFJ for her help with the preparation of the samples, and F. W. Hamburg and A. Mastenbroek of ECN for the determination of the thickness of the 0·005 mm crystal.

APPENDIX

In this Appendix, a more formal derivation will be given of the function Ψ. An expression for the general case will be given and the approximations discussed. For two special cases, symmetrical reflection and symmetrical transmission of an infinite plane parallel crystal plate, exact expressions for Ψ will be given.

General case

For crystals with a mosaic microstructure the power of the diffracted beam $I_B^{\pm}(\varepsilon)$ is given (Zachariasen, 1967) by:

$$I_B^{\pm}(\varepsilon)=\mathscr{I}_0 v\sigma^{\pm}(\varepsilon)\,\varphi[\sigma^{\pm}(\varepsilon)]. \qquad (A1)$$

The meaning of the symbols is the same as in Becker & Coppens (1974).

Inserting (A1) into the definition of the observable flipping ratio given by (2a) we obtain:

$$R_B(\varepsilon)=R\,\frac{\varphi[\sigma^+(\varepsilon)]}{\varphi[\sigma^-(\varepsilon)]}, \qquad (A2)$$

$$R=\sigma^+(\varepsilon)/\sigma^-(\varepsilon). \qquad (A3)$$

R is the secondary-extinction-free value for the flipping ratio which is angle independent for negligible primary extinction (see later in this Appendix).

Equations (A1), (A2), and (A3) determine the analytical form of the function Ψ defined by (7),

$$R_B(\varepsilon)=R\Psi[I_B^+(\varepsilon)]. \qquad (A4)$$

It can be seen that the analytical form of the function Ψ depends mainly on the form of the extinction function φ.

Becker & Coppens (1974) proved that in the general case this function can be approximated by a series expansion

$$\varphi(\sigma^{\pm})=\sum_{n=0}^{\infty}(-1)^n(\sigma^{\pm})^n\,\overline{T^n}/n!$$

$$=1-\sum_{n=1}^{\infty}(-1)^{n-1}(\sigma^{\pm})^n\,\overline{T^n}/n!, \qquad (A5)$$

with

$$\overline{T^n}=\int_v \mathrm{d}v\sum_{j=0}^{n}\binom{n}{j}^2 T_1^j\,T_2^{n-j}/V. \qquad (A6)$$

If $\sigma^{\pm}\bar{T}\ll 1$ we may approximate the extinction function by

$$\varphi[\sigma^{\pm}(\varepsilon)]=1-\sigma^{\pm}(\varepsilon)\,\bar{T}, \qquad (A7)$$

and function Ψ by

$$\Psi[I_B^+(\varepsilon)]=\frac{1-\sigma^+(\varepsilon)\,\bar{T}}{1-\sigma^-(\varepsilon)\,\bar{T}}\approx 1-[\sigma^+(\varepsilon)-\sigma^-(\varepsilon)]\,\bar{T}. \quad (A8)$$

Retaining only linear terms in (A1) we obtain

$$[\sigma^+(\varepsilon)-\sigma^-(\varepsilon)]\,\bar{T}=\frac{\bar{T}}{\mathscr{I}_0 v}\,[I_B^+(\varepsilon)-I_B^-(\varepsilon)] \quad (A9)$$

and we may write for $R_B(\varepsilon)$

$$R_B(\varepsilon)=R[1-G\Delta I(\varepsilon)], \qquad (A10)$$

where

$$G=\bar{T}/\mathscr{I}_0 v, \qquad (A11)$$

$$\Delta I(\varepsilon)=I_B^+(\varepsilon)-I_B^-(\varepsilon). \qquad (A12)$$

Expression ($A10$) is similar to the one postulated in (8). Parameter G is now defined in ($A11$).

The above derivation is valid under the following assumptions:

(1) the microstructure of the crystal is homogeneous and well approximated by the mosaic model,

(2) the divergence of the incoming beam is small relative to the width of the mosaic of the crystal,

(3) the condition $(\sigma^+ - \sigma^-)\bar{T} \ll 1$ is fulfilled,

(4) parameter R is angle independent, which means that primary extinction has to be negligible. This condition can be understood from the argument that the angular dependence of the neutron cross-section for perfectly ordered grains and the angular dependence arising from the crystal mosaic are different.

Symmetrical Bragg case

For the case of scattering by an infinite plane parallel crystal plate in the symmetrical reflection position, there is an exact solution for the extinction function φ (Zachariasen, 1967):

$$\varphi[\sigma^{\pm}(\varepsilon)] = 1/[1 + \sigma^{\pm}(\varepsilon)\bar{T}]. \qquad (A13)$$

By combination of this expression with ($A1$) one obtains

$$\varphi[\sigma^{\pm}(\varepsilon)] = 1 - GI_B^{\pm}(\varepsilon), \qquad (A14)$$

where G has the same meaning as in ($A11$). Substituting this in ($A2$) one arrives at

$$R_B(\varepsilon) = R[1 - GI_B^+(\varepsilon)]/[1 - GI_B^-(\varepsilon)]. \qquad (A15)$$

This expression can be converted into:

$$R_B(\varepsilon) = R\left\{1 - \frac{R - R_B(0)}{R}\frac{I_B^+(\varepsilon)}{I_B^+(0)}\right\}. \qquad (A16)$$

In this way the problem of deducing an expression for Ψ has been solved in an exact way independently of crystal thickness and the amount of secondary extinction.

Symmetrical Laue case

Also for the case of scattering by an infinite plane parallel crystal plate in symmetrical transmission an exact solution for φ has been given (Zachariasen, 1976):

$$\varphi[\sigma^{\pm}(\varepsilon)] = \frac{1 - \exp[-2\sigma^{\pm}(\varepsilon)\bar{T}]}{2\sigma^{\pm}(\varepsilon)\bar{T}}. \qquad (A17)$$

Combination of ($A17$) with ($A1$), ($A3$), and ($A11$) leads to:

$$\varphi[\sigma^+(\varepsilon)] = \frac{2GI_B^+(\varepsilon)}{\ln[1 - 2GI_B^+(\varepsilon)]}, \qquad (A18a)$$

$$\varphi[\sigma^-(\varepsilon)] = \frac{1 - [1 - 2GI_B^+(\varepsilon)]^{1/R}}{(1/R)\ln[1 - 2GI_B^+(\varepsilon)]}, \qquad (A18b)$$

and with ($A2$)

$$R_B(\varepsilon) = \frac{2GI_B^+(\varepsilon)}{1 - [1 - 2GI_B^+(\varepsilon)]^{1/R}}. \qquad (A19)$$

Expression ($A19$) represents the solution to the problem of finding an exact solution for Ψ in the symmetrical Laue case.

Remark

As already stated in the introduction of this paper, the amount of secondary extinction varies when a crystal is rotated through the Bragg peak. The use of polarized neutrons offers a unique possibility to detect this variation as a change in the observed flipping ratio $R_B(\varepsilon)$, a possibility that is not present when unpolarized neutrons are being used.

In order to investigate whether, for a given crystal, the Zachariasen model for secondary extinction is valid, the scattering power of the crystal has to be varied, which normally is done either by varying the wavelength or by using samples of different thickness.

The use of polarized neutrons, combined with measuring the R-on-rocking-curve offers a third possibility. For the employment of this possibility, an analytical formulation of the observable flipping ratio $R_B(\varepsilon)$ in terms of the extinction-free flipping ratio R, and the observed intensity $I_B^+(\varepsilon)$ is given in this Appendix. In the general case it is only possible to give a practical formulation ($A10$) for sufficiently thin crystals. For the symmetrical Laue and Bragg cases it turns out to be possible to deduce more general formulations, ($A16$) and ($A19$), that are also valid for thicker crystals.

References

Becker, P. J. & Coppens, P. (1974). *Acta Cryst.* A**30**, 129–147.

Bonnet, M., Delapalme, A., Becker, P. & Fuess, H. (1976). *Acta Cryst.* A**32**, 945–953.

Brun, T. O. & Lander, G. H. (1974). *Phys. Rev.* B**9**, 3003–3012.

Lander, G. H. & Brun, T. O. (1973). *Acta Cryst.* A**29**, 684–691.

Nathans, R., Shull, C. G., Shirane, G. & Andresen, A. F. (1959). *J. Phys. Chem. Solids*, **10**, 138–146.

Zachariasen, W. H. (1967). *Acta Cryst.* **23**, 558–563.